Analysis of the Kinetics of Diffraction Efficiency during the Holographic Grating Recording in Azobenzene Functionalized Polymers

ARTICLE *in* THE JOURNAL OF PHYSICAL CHEMISTRY B · MARCH 2007

Impact Factor: 3.3 · DOI: 10.1021/jp067021l · Source: PubMed

2 AUTHORS, INCLUDING:

Andrzej Miniewicz
Wroclaw University of Technology
223 PUBLICATIONS **1,848** CITATIONS

Analysis of the Kinetics of Diffraction Efficiency during the Holographic Grating Recording in Azobenzene Functionalized Polymers

Anna Sobolewska and Andrzej Miniewicz*

Institute of Physical and Theoretical Chemistry, Wroclaw University of Technology, Wybrzeze Wyspianskiego 27, 50-370 Wroclaw, Poland

Received: October 26, 2006; In Final Form: December 7, 2006

The laser-assisted holographic grating recording process in films of azobenzene functionalized polymers is usually studied by observation of the efficiency of light scattering on a developing in time diffraction grating. Various possible mechanisms contributing to grating formation as well as the bulk or surface origin (bulk refractive index and/or relief grating) of light scattering make the analysis of kinetics of grating recording, from the light scattering data only, difficult and ambiguous. To fully explain experimentally observed various and complex (frequently nonexponential) kinetics of the first-order light diffraction intensity, we considered a simple single-exponential growth of the two phase gratings in the same polymer film. In modeling we assumed that the bulk refractive index grating $\Delta n(t)$ and the surface relief grating $\Delta d(t)$ differ considerably in their growth rates and we allowed for a nonstationary phase shift $\Delta\varphi(t)$ between them which was experimentally observed during the recording process. The origin of the nonstationary phase shift is a result of a slow shift of interference pattern due to delicate symmetry breaking in illumination conditions (e.g., difference in beam intensities and deviation of exact symmetrical beam incidence angles on the sample). Changing only such parameters as stationary amplitudes of refractive index and relief gratings for a span of phase shifts ($0-\pi$) between them, we obtained a series of kinetic responses which we discuss and interpret. The various examples of temporal evolution of diffraction efficiency for the same grating formation kinetics, modeled in our work, supply evidence that great care must be taken to properly interpret the experimental results.

1. Introduction

Azobenzene functionalized polymers have been widely investigated in the past decade because of their potential use in different optical applications including optical information storage and processing, polarization holography, and various kinds of photonic devices.[1−6] Many of these applications rely on photoinduced anisotropy (PIA), which is a consequence of many efficient reversible trans−cis−trans photoisomerization cycles of azobenzene groups[5,7−11] initiated by absorbed polarized laser light. The process of the PIA is classically described by three consecutive mechanisms: angular hole burning, angular redistribution, and thermal angular diffusion.[9−11] These usually fast molecular orientation processes in azobenzene functionalized polymers are accompanied by much slower surface relief grating (SRG) formation.[4,6,7,12−24] The latter process, initiated by spatially periodic light illumination, is linked with pendent azo-group movements causing polymer chain migration, which results in free surface corrugation releasing accumulated stress in a viscoelastic medium. Both phenomena, i.e., PIA leading to bulk refractive index grating and SRG formation, occur simultaneously in azopolymers and are the subject of studies employing holographic techniques (cf. refs 24 and 25). The dynamics and the strength of these two effects during grating recording can be measured by observation of the first-order diffraction efficiency which generally is proportional to the square of the light induced phase amplitudes in a studied material. Additionally, SRGs are nowadays well characterized using atomic force microscopy[6,7,12−14,17−18,20−23] and phase shifts between light intensity pattern and phase or amplitude gratings are measured with the translation grating technique.[26]

In this work we propose a simple model of vectorial grating approach to explain the complex dynamics of photoinduced bulk and surface relief grating formation during holographic recording in azobenzene functionalized polymers. The diffraction efficiency of light scattered on in situ recorded gratings generally comes from two phase gratings and one amplitude grating. The latter one, the so-called absorption grating, is neglected in our considerations for clarity of presentation. The remaining phase gratings, i.e., a bulk refractive index grating and a surface relief grating, are due to refractive index modulation in the bulk of the material $\Delta n(t)$ and film thickness modulation $\Delta d(t)$, respectively. These two gratings show different temporal growth rates. At the beginning of the grating recording process, the refractive index grating dominates the diffraction as the amplitude of refractive index modulation rises quickly with time, being related to angular molecular redistribution. For longer exposures the surface relief grating, related to viscoelastic properties of the polymer, may give the strongest contribution to light diffraction due to higher attainable phase amplitudes. From our previous observations[25,27−31] and observations of other groups,[14,15,22,24,32−35] it was evident that during recording the phase shift between the above-mentioned gratings and light intensity pattern may arise. In most of the so far reported experiments this shift was either 0 or π, reflecting different surface corrugations with respect to the light intensity pattern in photochromic polymers ($\Delta\varphi = 0$) and photochromic liquid-

* Corresponding author. Telephone: (048) 71-320-35-00. Fax.: (048) 71-320-33-64. E-mail: andrzej.miniewicz@pwr.wroc.pl.

10.1021/jp067021l CCC: $37.00
Published on Web 01/31/2007

crystalline polymers ($\Delta\varphi = \pi$).[36] In his recent work Reinke et al.[32] introduced a simple model describing the dynamics of the holographic grating recording in an azo glass by assuming an arbitrary phase shift between the refractive index and the surface relief gratings and showed how the dynamics of diffraction efficiency growth is affected. However, it is difficult to propose a physical mechanism generating a stationary phase shift $\Delta\varphi$ = constant between the gratings which is different from 0 or π because such a process requires symmetry breaking. Assumption of the fixed-in-time phase shift between the gratings is an oversimplification of a real process. Therefore, in this work we wish to extend the approach of Reinke et al.[32] introducing the nonstationary phase shift $\Delta\varphi(t) \neq$ constant. One can mention at least three possible mechanisms leading to symmetry breaking during a degenerate two-wave mixing (holographic) experiment: (i) intensity difference between grating inscribing beams, (ii) nonequal beam incidence angles onto the sample surface, and (iii) the presence of the third laser beam used for monitoring of light diffraction efficiency which usually has an oblique incidence angle.

The first (i) mechanism is linked with the evolution in time of a relative phase difference between two coherent laser beams. This may occur as a result of slightly faster polymer bleaching and related to it refractive index change along the path of the stronger beam. The changing-in-time phase difference between the crossing beams produces the changing-in-time spatial shift of the interference pattern in one direction along the grating wave vector $\bar{k}$. The faster of the two grating buildup processes will partially follow this shift, while the slower of them will be retarded. This mechanism will produce a nonstationary phase shift between the bulk refractive index and relief gratings. A similar origin, i.e., different self-phase action of two coherent beams propagating in light-sensitive medium, was used by us to explain an efficient beam coupling occurring in methylene blue doped gelatin.[37] The speed of replacement of the light intensity pattern is usually faster at the beginning of the recording process and slows down for longer exposures, and its magnitude depends on the difference in light intensities and light path through sample thickness.

The second mechanism (ii) is in fact similar to the previously described (i), but the difference in phase between the grating recording beams occurs due to the difference in light paths related to sample tilting with respect to the beam bisectrice.

The third mechanism (iii) can be operative only if the reading beam illuminates the sample at an oblique angle and its light is absorbed and therefore introduces a refractive index change of the material. An evolution in time between amplitude and phase gratings was experimentally observed in azo-functionalized polymers by the translation grating technique[38] and also reported in refs 33 and 39. Therefore, in order to properly describe the light diffraction evolution with time, the time-dependent phase shift $\Delta\varphi(t)$ must be taken into consideration. From modeling, which will be shown in section 3, it follows that in many cases the phase shift between the gratings cannot be neglected. Its presence might be decisive for a proper understanding of the frequently observed nonexponential growths and possessing minima and maxima curves of diffraction efficiency as a function of recording time in azopolymers.

2. Theoretical Approach

We consider a thin film of azobenzene functionalized polymer deposited over a glass plate. In two-wave-mixing holographic grating recording experiment the film is set perpendicular to the *z*-axis and is illuminated by a pair of nominally equal intensity and linear polarization crossed laser beams lying in the $x-z$ plane and having bisectrice along the *z*-axis. The film is illuminated from its freestanding side. Assuming that the total light intensity incident on the sample $I(x)$ is sinusoidally modulated with the modulation factor $m = 1$, the spatial modulation of the refractive index $n(x,t)$ along the *x*-axis and a film thickness $d(x,t)$ in the linear approximation are expected to have the forms:

$$n(x,t) = n_0 + \frac{\Delta n(t)}{2}\cos\left(\frac{2\pi}{\Lambda}x\right) \quad (1)$$

$$d(x,t) = d_0 + \frac{\Delta d(t)}{2}\cos\left(\frac{2\pi}{\Lambda}x + \Delta\varphi(t)\right) \quad (2)$$

where $\Delta n/2$ and $\Delta d/2$ are the amplitudes of the bulk refractive index and the surface relief grating, respectively, n_0 is the average refractive index of the polymer at the respective light wavelength λ, and d_0 is the polymer thickness prior illumination. Λ is the period of light-induced diffraction grating determined by the angle θ between the recording beams, $\Lambda = (\lambda/2)\sin(\theta/2)$; $\Delta\varphi(t)$is the phase shift between the two gratings.

For relatively thin polymeric films the multiple-order light self-diffraction is observed during holographic grating recording (a Raman−Nath light scattering regime). The process of grating buildup could be monitored with another laser beam, incident at an oblique incidence angle α,[40] by observation of light power scattered into first diffraction order. The reading laser beam should be weak in power and have a different red-shifted wavelength in order to minimize the deterioration of the grating recording process occurring at resonance laser excitation. In such a case, for the pure phase grating, the first-order diffraction efficiency $\eta_1(t)$, defined as the ratio between the first-order diffracted beam intensity $I_{1\text{diff}}(t)$ and the single input beam intensity $I_0(t)$, is described by the square of the first-order Bessel function J_1:[40]

$$\eta_1(t) = \frac{I_{1\text{diff}}(t)}{I_0(t)} = J_1^2(\Delta\phi(t)) \quad (3)$$

where $\Delta\phi(t)$ is the maximum phase retardation accumulated by a plane wave of wavelength λ transmitted through the system. $\Delta\phi(t)$ is the sum of phase retardations $\Delta\phi_n(t)$ and $\Delta\phi_d(t)$ due to the bulk refractive index and the surface relief gratings, assuming that there is no phase shift $\Delta\varphi$ between them:

$$\Delta\phi_n(t) = \frac{2\pi(\Delta n(t))d_0}{\lambda\cos(\alpha)} \quad (4)$$

$$\Delta\phi_d(t) = \frac{2\pi(\Delta d(t))n_{\text{eff}}}{\lambda\cos(\alpha)} \quad (5)$$

where n_{eff} is the effective refractive index of a corrugated layer (polymer + air) and is estimated using the Maxwell−Garnett approximation as $n_{\text{eff}} \approx (1 + n_0)/2$.[41]

In general this approach is not sufficient to properly describe these cases when the above-mentioned gratings are shifted in phase $\Delta\varphi$ with respect to each other, as is shown in Scheme 1.

In such a case the simple vectorial grating approach is more appropriate. Following the idea proposed by Reinke et al.,[32] both gratings are treated as vectors in two-dimensional space with an angle between them described by $\Delta\varphi$. The modulus of an effective phase retardation vector $\Delta\phi(t)$ is given by the grating phase retardations $\Delta\phi_n(t)$ and $\Delta\phi_d(t)$ and an angle $\Delta\varphi$. In our analysis of temporal evolution of diffraction efficiency observed

SCHEME 1: Schematic Illustration of the Sinusoidal Bulk Refractive Index, Δn, and the Surface Relief, Δd, Gratings, and Related Phase Parameters, $\Delta\phi_n$ and $\Delta\phi_d$[a]

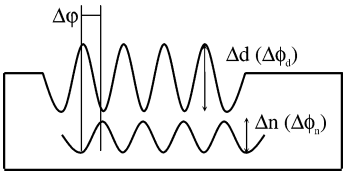

[a] The phase shift $\Delta\varphi$ between the gratings is also indicated.

for an in situ recorded gratings, we extend the model proposed by Reinke et al.[32] in that aspect that besides $\Delta n(t)$ and $\Delta d(t)$ we allow for time-dependent phase shift $\Delta\varphi(t)$ between the gratings as was discussed earlier. Having this in mind, the first-order diffraction efficiency is described by the expression

$$\eta_1(t) = J_1^2\{2\pi[((\Delta n(t))d_0)^2 + (\Delta d(t)n_{\text{eff}})^2 + 2(\Delta n(t))d_0(\Delta d(t))n_{\text{eff}}\cos(\Delta\varphi(t))]^{1/2}[\lambda\cos(\alpha)]^{-1}\} \quad (6)$$

We assume that the dynamics of two processes, i.e., refractive index and surface relief grating formation in azopolymers upon constant light illumination $\Delta n(t)$ and $\Delta d(t)$, respectively, is described by the single-exponential functions of the form

$$\Delta n(t) = \Delta n_{\max}[1 - \exp(-t/\tau_1)] \quad (7)$$

$$\Delta d(t) = \Delta d_{\max}[1 - \exp(-t/\tau_2)] \quad (8)$$

where τ_1 and τ_2 are the characteristic grating formation time constants, and $\Delta n_{\max}$ and $\Delta d_{\max}$ are the maximum refractive index and thickness modulations, respectively, for given experimental conditions, i.e., light intensity, wavelength, grating period, sample thickness, and polymer type. Throughout this work we assumed a single kinetics of grating growth determined by time constants $\tau_1 = 100$ s and $\tau_2 = 1500$ s. The selected values of physical constants are typical for azo-functionalized polymers with respect to the observed evolution of relief and bulk refractive index grating buildup processes when the continuous-wave Ar^+ laser is used as an excitation source ($\lambda =$ 514.5 nm, 10 mW single beam power, 1.5 mm beam diameter). The resulting mass transport of polymer and formation of substantial SRG is on the order of 1000−3000 s and is related to the glass transition temperature T_g of polymer. The plots of a normalized bulk refractive index coefficient $\Delta n(t)/\Delta n_{\max}$ and a surface relief modulation $\Delta d(t)/\Delta d_{\max}$ for these time constants are shown in Figure 1 in the time interval 0−6000 s. Expressions 7 and 8 describe a natural tendency of reaching saturation of any material parameter for infinite exposure time. However, a coupling between bulk molecular reorientation of azo moieties and polymer chain movements initiated by the former process must certainly exist. Therefore, the time constant of the faster process τ_1 describing the rate of angular molecular redistribution and the slower one τ_2 describing the process of polymer mass transport resulting in a surface corrugation are indirectly related to each other. Moreover, slow mass transport unable to follow the light intensity pattern shift is the main reason for the refractive index versus relief grating phase shift $\Delta\varphi(t)$.

To model the possible temporal behavior of the phase shift between the gratings $\Delta\varphi(t)$, the dependence of the ratio $\Delta\phi_n(t)/\Delta\phi_d(t)$ was monitored for $\tau_1/\tau_2 = 1/15$. We concluded that in this particular case the expression describing the dynamics of $\Delta\varphi(t)$ would be the double-exponential growth function:

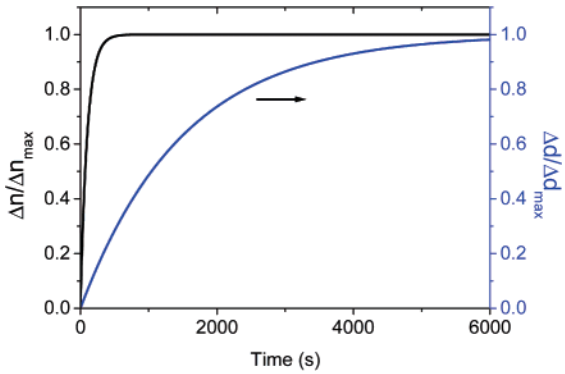

Figure 1. Normalized bulk refractive index grating amplitude and normalized relief amplitude as a function of time. The assumed values for the modeling time constants are $\tau_1 = 100$ s (refractive index grating) and $\tau_2 = 1500$ s (relief grating).

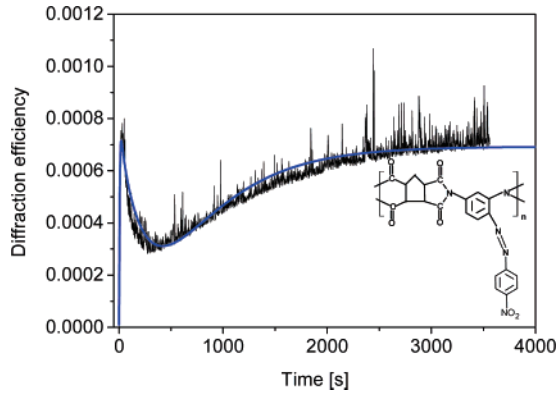

Figure 2. Experimentally measured self-diffraction efficiency as a function of time for cycloaliphatic−aromatic polyimide. The chemical structure of the polyimide is shown in the figure. The solid line represents the fit of the experimental data with the vectorial grating model. The noise is connected to the mechanical instability shifting temporarily light interference pattern with respect to the existing grating and leading to beam coupling.

$$\Delta\varphi(t) = (\Delta\varphi_{\max}(\infty))\{A[1 - \exp(-t/\tau_A)] + B[1 - \exp(-t/\tau_B)]\} \quad (9)$$

where the sum of parameters A and B fulfills the condition $A + B = 1$, and τ_A and τ_B are the time constants (here we assumed $\tau_A = 166$ s, $\tau_B = 808$ s). This expression is arbitrary, but it reflects the compromise between saturation behavior of the origin of phase shift (photobleaching) and the dynamics of cooperative molecular processes related to grating buildup. The form of the $\Delta\varphi(t)$ function for given experimental conditions can be established experimentally with the grating translation technique applied in sequence during the grating recording process.[38] By the introduction of the time-dependent phase shift (cf. eq 9) the limitation of the model approach proposed by Reinke el at.,[32] i.e., the assumption that the phase shift between the gratings is fixed, was released. This opens a possibility to cover more cases of experimentally observed temporal evolution of diffraction efficiency in azo-functionalized polymers.

3. Results and Discussion

The inspiration of the present work was the will to describe what is frequently observed in self-diffraction experiments in azobenzene functionalized polymers—a temporal behavior of the first-order diffraction efficiency composed of an initial rise followed by the decrease and subsequent growth to the saturation value. An example of such untypical behavior is shown in Figure

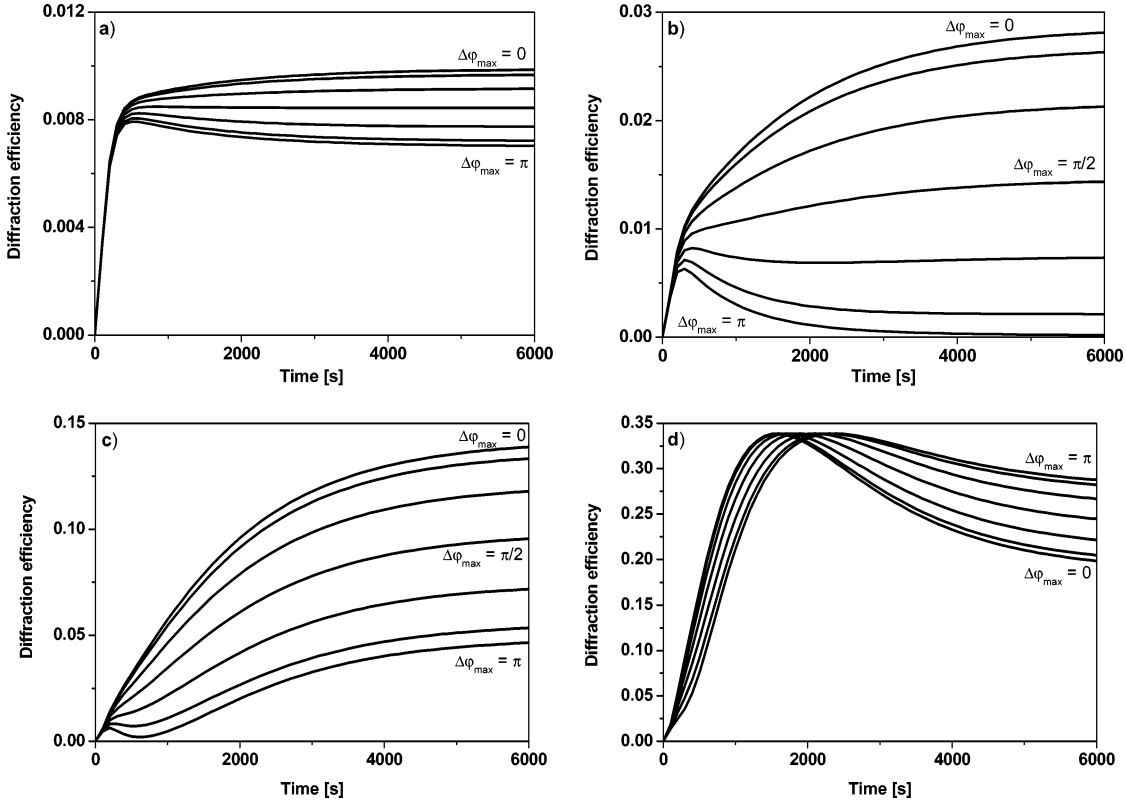

Figure 3. Diffraction efficiencies as a function of time calculated for relatively small bulk refractive index modulation $\Delta n_{max} = 0.015$ and different phase shifts between the gratings $\Delta\varphi_{max} = 0$, $\pi/6$, $\pi/3$, $\pi/2$, $2\pi/3$, $5\pi/6$, and π. Surface relief modulations Δd_{max}: (a) 1, (b) 10, (c) 40, and (d) 160 nm.

2 for cycloaliphatic−aromatic polyimide characterized by T_g > 300 °C[30] and giving quite permanent surface relief gratings under s−s polarization of recording light.

Below, a series of numerical results of diffraction efficiency as a function of time $\eta_1(t)$ obtained for different parameters and calculated according to expression 6 are presented. We varied the maximum (saturation) values of the amplitude of induced refractive index modulation, the amplitude of thickness modulation, and the phase shift between them. All the results were obtained for the same set of grating growth time constants: $\tau_1 = 100$ s and $\tau_2 = 1500$ s. These values were typical ones obtained in a real experiment. For clarity of the presentation we assumed a typical thickness of the polymeric film $d_0 = 1000$ nm. We took the typical refractive index at $\lambda = 514.5$ nm as $n_0 = 1.600$, which led to the effective refractive index, used in calculations of the diffraction efficiency of the relief grating, $n_{eff} = 1.300$; we also assumed that the angle was equal to $\alpha = 10°$. The numerical simulations were performed for two quantitatively different cases:

(i) The first case was a relatively small ($\Delta n_{max} = 0.015$) maximum bulk refractive index modulation amplitude and a set of the maximum thickness modulation amplitudes $\Delta d_{max} = 1$, 5, 10, 20, 40, 80, 120, and 160 nm.

(ii) The second case was a relatively large ($\Delta n_{max} = 0.1$) maximum bulk refractive index modulation amplitude and the thickness modulation amplitude as in case i.

The choice of the above parameters and cases is rationalized in Table 1 where calculated light phase retardations for the bulk refractive index grating $\Delta\phi_n$ and the surface relief grating $\Delta\phi_d$ cover two possible cases of dominance with respect to light diffraction of one or another grating.

In simulations we allow that the maximum phase difference between the gratings took different values in the range $(0, \pi)$:

TABLE 1: Modeling Parameters: Maximum Bulk Refractive Index, Δn_{max}, and Surface Relief, Δd_{max}, Grating Modulations and Related Phase Shifts, $\Delta\phi_n$ and $\Delta\phi_d$, Due to These Gratings for $d_0 = 1$ μm and $n_0 = 1.600$

Δn_{max}	$\Delta\phi_n$ [rad]	Δd_{max} [nm]	$\Delta\phi_d$ [rad]
0.015	0.184	1	0.016
		10	0.156
		40	0.626
		160	2.503
0.1	1.226	1	0.016
		20	0.301
		80	1.252
		160	2.503

$\Delta\varphi_{max}(\infty) = 0$, $\pi/6$, $2\pi/6$, $3\pi/6$, $4\pi/6$, $6\pi/6$, and π. The values of the time constants used in eq 9 were $\tau_A = 808$ s and $\tau_B = 166$ s. The final diffraction efficiency depends on the duration of the recording process. In simulation we assumed that the films were exposed to the interference light during a period of 6000 s.

3.1. Low Bulk Refractive Index Amplitude Grating $\Delta n_{max} = 0.015$. In Figure 3 we have shown how the phase shift between the gratings changing as a function of time $\Delta\varphi(t)$ influences the dynamics of the first-order light diffraction signal. The graphs were plotted for four different cases: (i) the total phase retardation $\Delta\phi(t)$ was dominated by the bulk refractive index grating contribution (the $\Delta\phi_n(t)$ was more than 10 times larger than the phase retardation due to surface relief grating $\Delta\phi_d(t)$, Figure 3a); (ii) the contribution of both phase retardations was comparable $\Delta\phi_n(t) \sim \Delta\phi_d(t)$ (Figure 3b); (iii) the phase retardation due to the surface relief grating $\Delta\phi_d(t)$ started to dominate (Figure 3c); (iv) the $\Delta\phi(t)$ was considerably dominated by the $\Delta\phi_d(t)$ (Figure 3d). Refer also to Table 1, where the values of the phase retardations $\Delta\phi_n(t)$ and $\Delta\phi_d(t)$ are gathered.

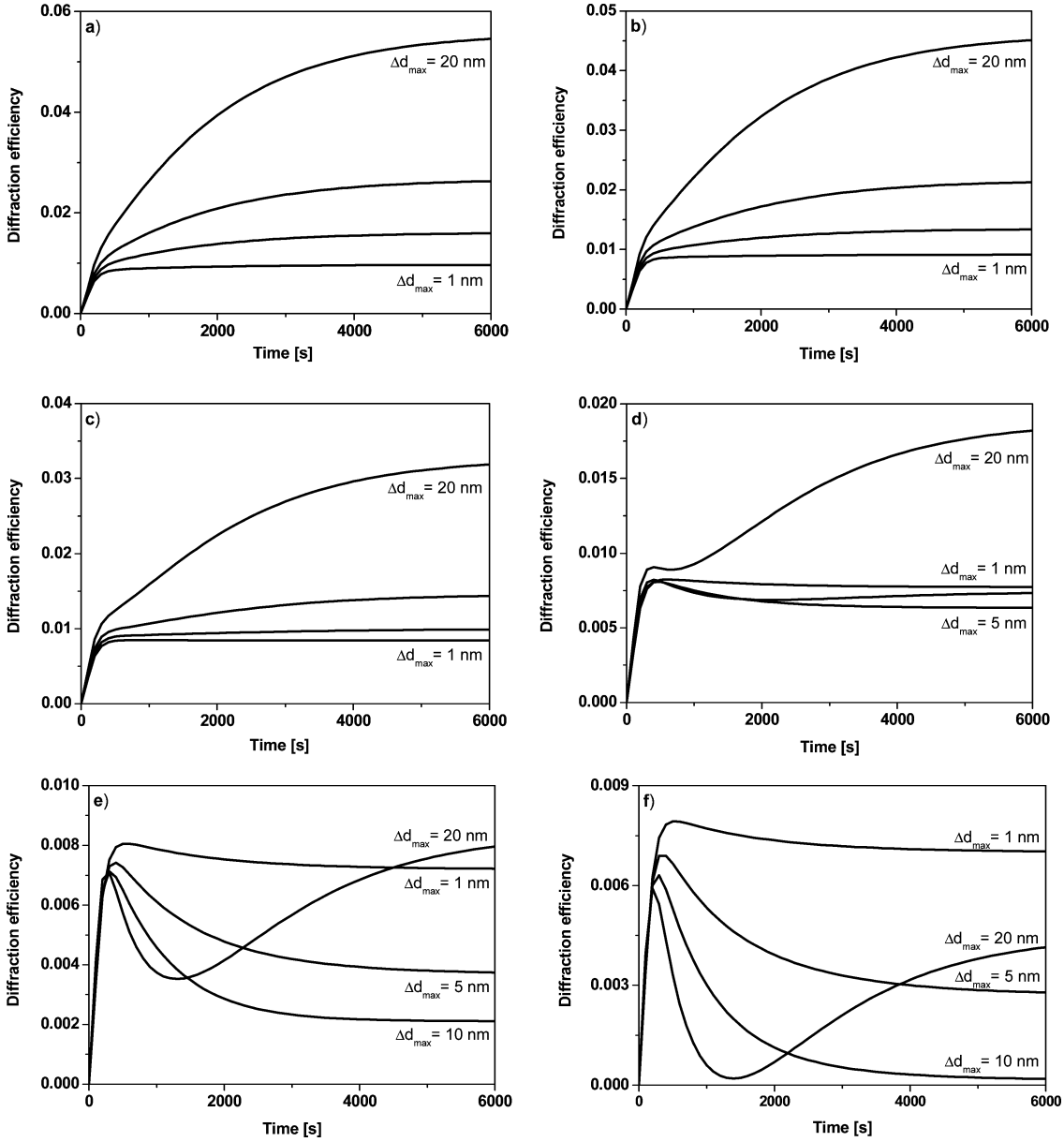

Figure 4. Diffraction efficiencies as a function of time obtained for different maximum surface relief modulations $\Delta d_{max} = 1$, 5, 10, and 20 nm for a fixed maximum bulk refractive index modulation $\Delta n_{max} = 0.015$ and various phase shifts between the gratings $\Delta\varphi_{max}$: (a) $\pi/6$, (b) $\pi/3$, (c) $\pi/2$, (d) $2\pi/3$, (e) $5\pi/6$, and (f) π.

When the bulk refractive index grating dominates the light diffraction (Figure 3a), the dynamics of the measured signal shows quasi-exponential growth and the phase shift between the gratings $\Delta\varphi_{max}$ does not considerably influence the light diffraction dynamics. Generally, diffraction efficiency is small, below 1%. The slight decrease in diffraction efficiency is observed after the saturation value due to bulk response (i.e., around $t = 200$ s) is reached; this decrease becomes visible for larger $\Delta\varphi_{max} > \pi/2$. In Figure 3b we present simulations performed for the case when the contribution to light diffraction coming from the both gratings is comparable. Diffraction efficiency for the most favorable case, when both contributions to light diffraction sum up, rises to nearly 3% and in a less favorable case is smaller than 1%. It is well seen that the phase shift between the gratings has a considerable effect on the dynamics of the diffraction efficiency. For $\Delta\varphi_{max}$ larger than $2\pi/3$ a significant decrease in the $\eta_1(t)$ starts to be observed, and for $\Delta\varphi_{max} = \pi$ the diffraction efficiency at prolonged exposure drops to much smaller values than 0.1%. The curves of $\eta_1(t)$ plotted in Figure 3c show how the phase shift between the gratings influences the dynamics of light diffraction when the phase shift due to the surface relief grating gives the dominating contribution to the light scattering process. The overall diffraction efficiency already for 40 nm amplitude of relief reaches nearly 15%. The dominance of light scattering on surface is compensated by the bulk refractive index modulation in initial time periods and for large $\Delta\varphi_{max}$ values. In some time interval it happens that the diffraction efficiency nearly drops to zero in value. When $\Delta\varphi_{max}$ is smaller than $\pi/2$, the dynamics of grating recording looks similarly to the case when contribution of both gratings were comparable with the only difference in the maximum value of the diffraction efficiency (the larger surface modulation causes the fast rise of the saturation value of $\eta_1(t)$).

The last case considered by us is when the relief grating has so huge an amplitude (here $\Delta d_{max} = 160$ nm) that it totally dominates the light scattering process. In such a case different phase shifts between two gratings have practically negligible

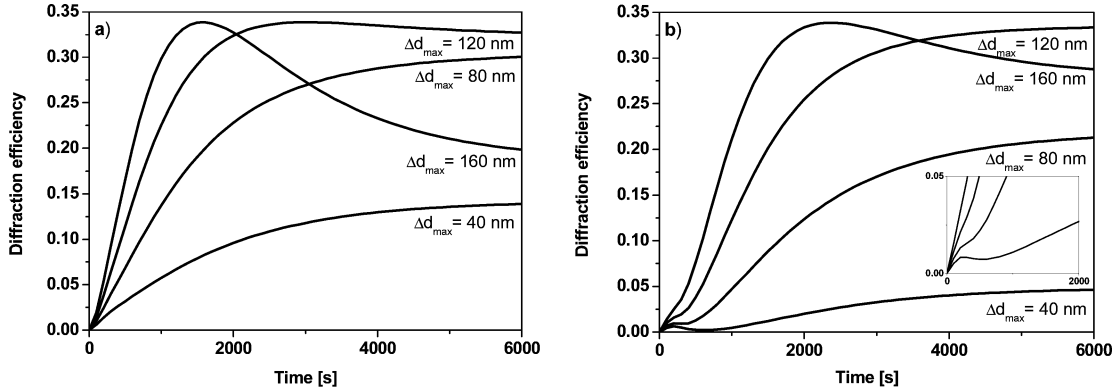

Figure 5. Diffraction efficiencies obtained for different maximum surface relief modulations $\Delta d_{max} = 40$, 80, 120, and 160 nm and maximum bulk refractive index modulation $\Delta n_{max} = 0.015$. (a) The gratings are in phase $\Delta\varphi_{max} = 0$, and (b) the gratings are out of phase $\Delta\varphi_{max} = \pi$. Inset shows initial recording period 0−2000 s.

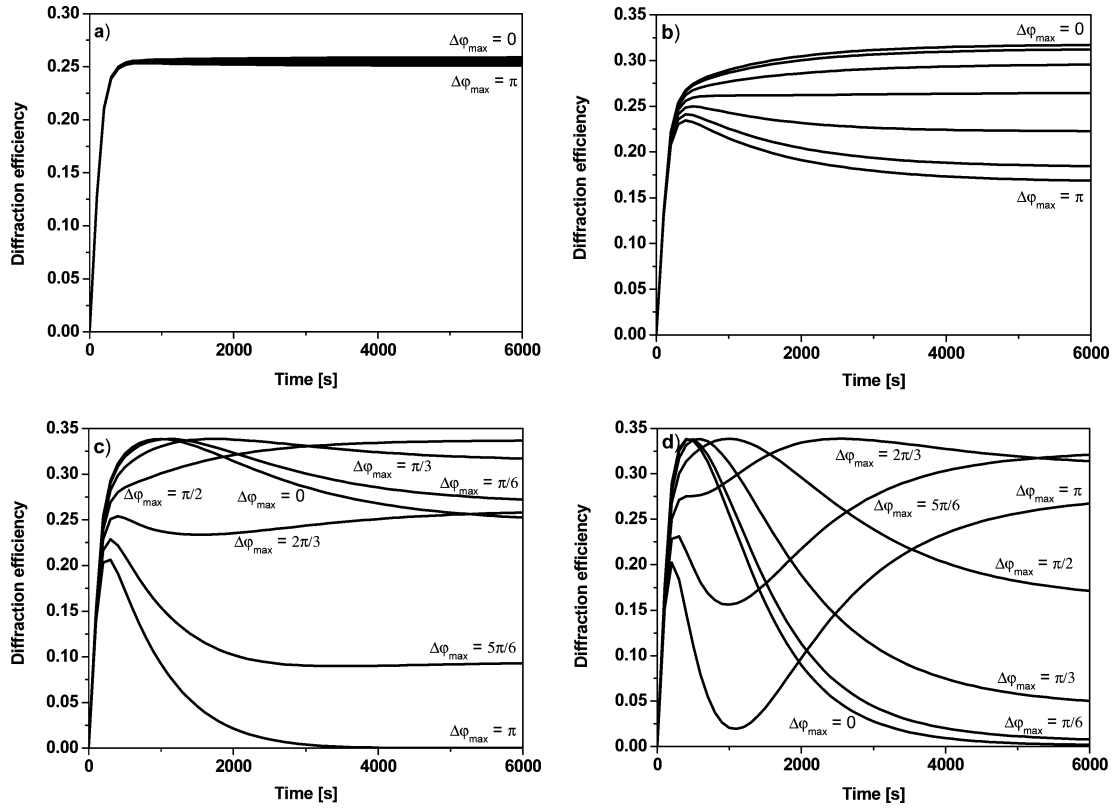

Figure 6. Diffraction efficiencies as a function of time calculated for a large maximum bulk refractive index modulation $\Delta n_{max} = 0.1$ and different phase shifts between the gratings $\Delta\varphi_{max} = 0$, $\pi/6$, $\pi/3$, $\pi/2$, $2\pi/3$, $5\pi/6$, and π. Surface relief modulations Δd_{max}: (a) 1, (b) 20, (c) 80, and (d) 160 nm.

influence on diffraction signal kinetics (Figure 3d). All the plotted curves look similar. The diffraction efficiency reaches the maximum $\eta_{1,max} = 33.9\%$ for $\Delta\phi \approx 1.8$ rad, which is strictly determined by the Bessel function properties for any kind of sinusoidal phase grating. When light phase retardation on the relief grating attains still higher values, the $\eta_1(t)$ starts to decrease in accordance with the square of the Bessel function plot. It is noteworthy that in real experiments the so-high values of diffraction efficiency in azopolymers are rarely observed due to the fact that materials of this type show absorption in the visible spectral range.

Now we numerically simulate the kinetics of light diffraction efficiency when bulk refractive index and relief grating contributions are more or less comparable, but we will analyze it for the cases with different phase shifts between the gratings. In Figure 4 there are six different graphs. In each graph the saturation value of the refractive index grating modulation is the same, $\Delta n_{max} = 0.015$, and the maximum surface modulation amplitude changes, $\Delta d_{max} = 1$, 5, 10, and 20 nm. Diffraction efficiencies simulated for different values of the phase shift between the gratings, $\Delta\varphi_{max}(t) = \pi/6$, $\pi/3$, $\pi/2$, $2\pi/3$, $5\pi/6$, and π, are plotted on individual graphs. It is seen that there is no difference in the shape of the curves of diffraction efficiencies $\eta_1(t)$ when $\Delta\varphi_{max}$ is smaller than $\pi/2$ (Figure 4a−c) even for surface relief grating modulations as large as $\Delta d_{max} = 20$ nm. The only observed difference is the position in time of the apparent maximum of diffraction efficiency. It appears earlier when the phase shift between the gratings increases. It is also observed that the saturation values of the $\eta_1(t)$ need more recording time when the surface relief grating modulation is higher. The distinct changes in shape of the $\eta_1(t)$ function become visible for the values of phase shift between the gratings

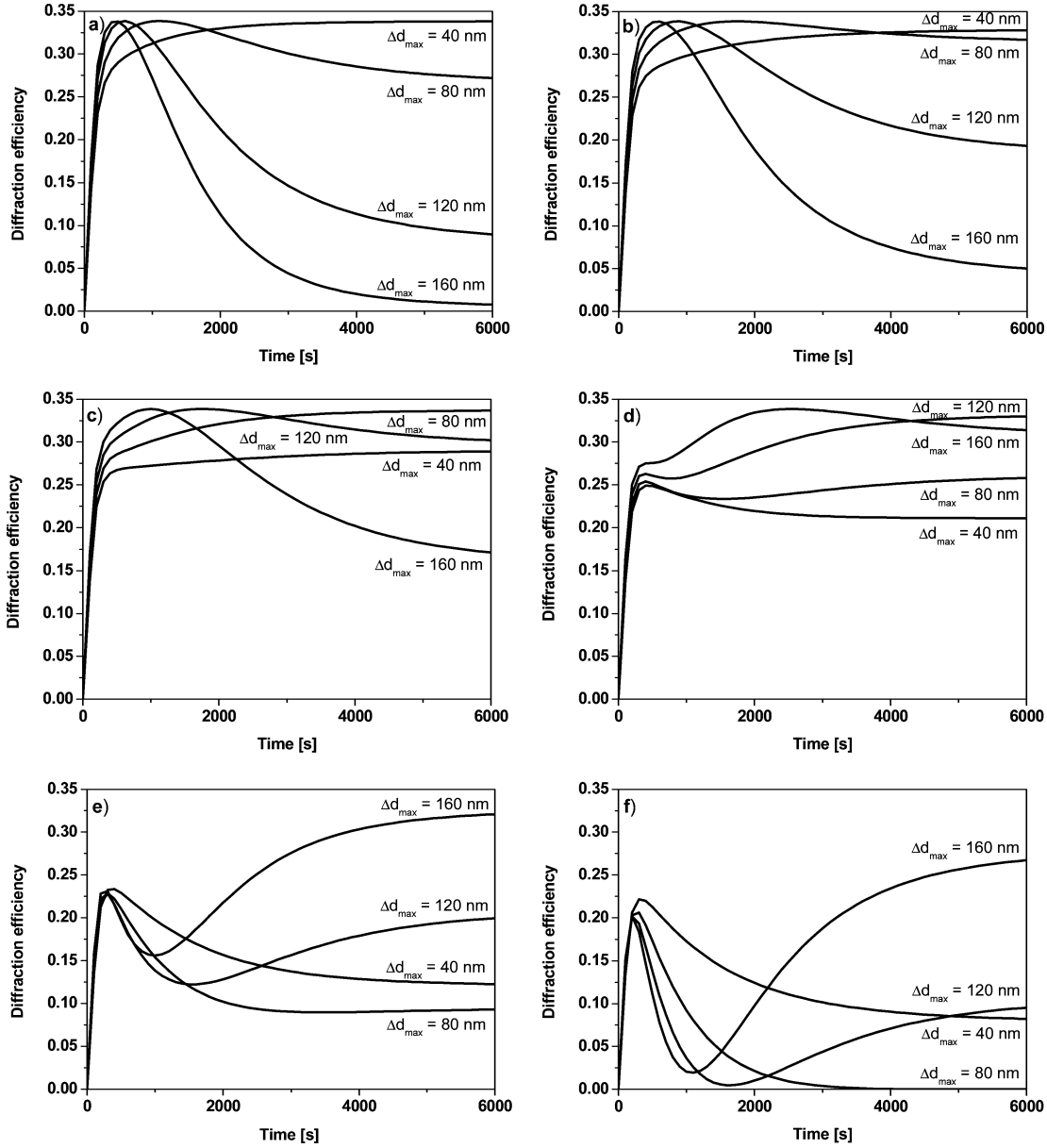

Figure 7. Diffraction efficiencies obtained for large surface relief modulation $\Delta d_{max} = 40$, 80, 120, and 160 nm and large bulk refractive index modulation $\Delta n_{max} = 0.1$. Phase shift between the gratings $\Delta\varphi_{max}$: (a) $\pi/6$, (b) $\pi/3$, (c) $\pi/2$, (d) $2\pi/3$, (e) $5\pi/6$, and (f) π.

lying within the range $\pi/2 < \Delta\varphi_{max}(t) \leq \pi$ (cf. Figure 4d−f). Especially for $\Delta d_{max} = 20$ nm there is a well-seen decrease of diffraction efficiency followed by a subsequent increase. The depth of the minimum of diffraction efficiency strongly depends on the phase shift between the gratings, and it is largest when the gratings are completely out of phase, i.e., $\Delta\varphi_{max} = \pi$ (cf. Figure 4f). The reason the dynamics of $\eta_1(t)$ looks so different for $\Delta d_{max} = 20$ nm is the fact that for this specific value of Δd_{max} both contributions to the total phase retardation $\Delta\phi(t)$ are comparable in magnitude.

In Figure 5 we have shown cases of higher relief grating amplitudes $\Delta d_{max} = 40$, 80, 120, and 160 nm. The curves of $\eta_1(t)$ were plotted only for two opposite cases of no phase shift ($\Delta\varphi_{max} = 0$) and a phase shift equal to π. It is seen that when light phase retardation $\Delta\phi_d(t) \gg \Delta\phi_n(t)$, i.e., $\Delta d_{max} = 120$ and 160 nm, the shapes of diffraction efficiency temporal evolutions look similar. They reach the absolute maximum diffraction efficiency in accordance with the Bessel function properties as described above. The effect of the opposite phases of the gratings on the dynamics of $\eta_1(t)$ is clearly observed for $\Delta d_{max} = 40$ and 80 nm with a noticeable minimum at the beginning of the recording. In the latter case the total diffraction efficiency is always smaller than in the case of gratings with $\Delta\varphi_{max} = 0$.

3.2. Large Bulk Refractive Index Amplitude Grating $\Delta n_{max} = 0.1$. In Figure 6 it is shown how the phase shift between the gratings influences the dynamics of the $\eta_1(t)$ when the maximum refractive index grating modulation is relatively large, i.e., $\Delta n_{max} = 0.1$. The analyses were performed for four different cases. Similarly to considerations described in the previous section, the phase retardation $\Delta\phi(t)$ influence was negligible for small relief amplitude $\Delta d_{max} = 1$ nm (cf. Figure 6a) and slightly greater for $\Delta d_{max} = 20$ nm (cf. Figure 6b). With the rise of relief grating importance the contributions to the light diffraction coming from both gratings become comparable (Figure 6c,d) and the magnitude $\Delta\phi(t)$ varies strongly with phase shift between the gratings, which is reflected in the evolution of $\eta_1(t)$.

The phase shift between the gratings has almost no influence on the dynamics of the diffraction efficiency when the bulk refractive index grating dominates the relief one ($\Delta\phi_n(t)$ is more

than 70 times larger than $\Delta\phi_d(t)$, see Table 1 and Figure 6a). In this case the diffraction efficiency curves show very fast exponential growth (related to τ_1). When the surface relief grating starts to appear (Figure 6b), the phase shift $\Delta\varphi$ has an influence on the $\eta_1(t)$ dynamics. For the highest $\Delta\varphi_{max} = \pi$, the largest decrease in the $\eta_1(t)$ is observed. The curves plotted in Figure 6c represent cases when the contributions of both gratings to the diffraction efficiency are comparable. In such cases the phase shift between the gratings has a weak effect on the dynamics of the $\eta_1(t)$. For $\Delta\varphi_{max} = 0$ and $\pi/6$ the absolute maximum of diffraction efficiency ($\eta_{max} = 33.9\%$) due to Bessel function properties is observed, and after that the $\eta_1(t)$ slowly decreases. However, for $\Delta\varphi_{max} = \pi/2$ one gets only a double-exponential growth function which smoothly changes into a curve with a single maximum for larger $\Delta\varphi_{max}$ values and $\eta_1(t)$ drops to zero for out-of-phase gratings of equal phase retardation amplitudes. The most spectacular changes in $\eta_1(t)$ are seen in Figure 6d, i.e., when the phase shift due to surface relief grating dominates the diffraction at longer times. Especially interesting curves are obtained for $\Delta\varphi_{max} = 5\pi/6$ and π. The sharp peak of $\eta_1(t)$ is followed by a deep minimum, and again the diffraction rises approximately with the time constant characteristic for relief formation. This is a typical behavior in all polymeric samples with a strong dominance of relief grating (cf. Figure 2).

In the series of figures shown in Figure 7 we compare all characteristic cases for the various maximum phase shifts between the gratings $\Delta\varphi_{max} = \pi/6$, $\pi/3$, $\pi/2$, $2\pi/3$, $5\pi/6$, and π. The value of the maximum bulk refractive index modulation was fixed at $\Delta n_{max} = 0.1$, and the maximum surface relief modulation varied as $\Delta d_{max} = 40$, 80, 420, and 160 nm. When $\Delta\varphi_{max} \leq \pi/2$ (Figure 7a−c) the two general types of the diffraction efficiency curves can be distinguished. The first one is when $\eta_1(t)$ rapidly increases at the beginning of the recording and after reaching a maximum monotonically decreases (cf. cases with $\Delta d_{max} = 120$ and 160 nm). The second one is described by a more or less deformed biexponential growth function with noticeable distortions of the $\eta_1(t)$ curve. When the maximum phase shift between the gratings is higher than $\pi/2$ (cf. Figure 7d−f), the plotted $\eta_1(t)$ curves look different. One can observe initially a maximum followed by a minimum and subsequent monotonic increase. Sometime this increase is suppressed.

The performed numerical simulations demonstrate how different diffraction responses can be measured for different polymeric materials. Having hundreds of light diffraction dynamic measurements in azo-functionalized polymers, we find that in the literature mostly those results are presented which show smooth biexponential growth. However, the plots shown in this analysis convinced us that the proper interpretation of other apparently complex experimentally observed $\eta_1(t)$ curves can be performed as well. Using our modeling, we fit the experimental curve shown in Figure 2 with the following parameters: $\tau_1 = 5$ s, $\tau_2 = 570$ s, $\Delta n_{max} = 0.0049$, $\Delta d_{max} = 5.1$, $\tau_A = 20$ s, $\tau_B = 1.5$ s, and $\Delta\varphi_{max} = 0.8\ \pi$.

One additional comment should be made at the end of these studies. In our modeling we took the excitation laser wavelength as $\lambda = 514.5$ nm. This wavelength usually lies within an absorption band of the azobenzene groups; thus the light is strongly absorbed. It is obvious that light absorption influences the value of the measured diffraction efficiency. Therefore, when comparing the results obtained here with those from an experiment, one should always take into account absorption losses; i.e., $\eta_1(t) = \exp[-(\alpha_{av}(\lambda))d_0]\ J_1^2(\Delta\phi(t))$, where $\alpha_{av}(\lambda)$ is the average sample absorption coefficient. We omitted absorption in our theoretical analysis because it does not influence the dynamics of the diffraction efficiency, causing only apparent lowering of $\eta_1(t)$.

4. Conclusions

Calculated hypothetical dynamics of diffraction efficiency during grating recording for different bulk refractive index and surface relief modulations and time-dependent phase shifts lead to following conclusions:

(a) The dynamics of grating recording in azopolymers strongly depends on the phase shift between the gratings.

(b) The influence of the phase shift is decisive on light diffraction when the contributions of both gratings to this process are comparable.

(c) The nonexponential and complex diffraction efficiency dependence on time observed experimentally (especially with maximum and minimum) could indicate the coexistence of two phase gratings of similar diffraction strengths shifted in phase.

The presented calculations, by assumption of the phase shift between the volume and surface gratings changing with time, predict and explain unusual dynamics of light diffraction efficiency. It was clearly shown that the phase shift between the gratings could not be neglected in all those cases in which efficient relief gratings are formed. The calculations performed by us are helpful in understanding the mechanisms of grating recording in azopolymers, either those experimentally observed by us[25,27−31] or those reported by other research groups.[14,15,22,24,32−35]

Acknowledgment. The authors wish to thank the Polish Ministry of Science and Higher Education for financial support under Grant 3 T08E 076 29 (A.S.) and Grant N507 132 31/3302 (A.M.).

References and Notes

(1) Kawata, Y.; Kawata, S. In *Photoreactive Organic Thin Films*; Sekkat, Z., Knoll, W., Eds.; Academic Press: San Diego, 2002; Chapter 16, p 514.
(2) Hagen, R.; Bieringer, T. *Adv. Mater.* **2001**, *13*, 1805.
(3) Kawata, S.; Kawata, Y. *Chem. Rev.* **2000**, *100*, 1777.
(4) Munakata, K.; Harada, K.; Itoh, M.; Umegaki, S.; Yatagai, T. *Opt. Commun.* **2001**, *191*, 15.
(5) Blanche, P.-A.; Lemaire, Ph. C.; Maertens, C.; Dubois, P.; Jérôme, R. *Opt. Commun.* **2000**, *185*, 1.
(6) Nathanson, A.; Rochon, P. *Adv. Mater.* **1999**, *11*, 1387.
(7) Delaire, J. A.; Nakatani, K. *Chem. Rev.* **2000**, *100*, 1817.
(8) Sekkat, Z. In *Photoreactive Organic Thin Films*; Sekkat, Z., Knoll, W., Eds.; Academic Press: San Diego, 2002; Chapter 3, p 64.
(9) Dumont, M.; Sekkat, Z.; Loucif-Saibi, P.; Nakatani, K.; Delaire, J. *Nonlinear Opt.* **1993**, *5*, 395.
(10) Dumont, M. *Nonlinear Opt.* **1996**, *15*, 69.
(11) Dumont, M.; El Osman, A. *Chem. Phys.* **1999**, *245*, 437.
(12) Kim, D. Y.; Tripathy, S. K.; Li, L.; Kumar, J. *Appl. Phys. Lett.* **1995**, *66*, 1166.
(13) Rochon, P.; Batalla, E.; Natansohn, A. *Appl. Phys. Lett.* **1995**, *66*, 136.
(14) Barrett, C.; Natansohn, A.; Rochon, P. *J. Phys. Chem.* **1996**, *100*, 8836.
(15) Jiang, X. L.; Li, L.; Kumar, J.; Kim, D. Y.; Shivshankar, V.; Tripathy, S. K. *Appl. Phys. Lett.* **1996**, *68*, 2618.
(16) Kumar, J.; Li, L.; Jiang, X.; Kim, D.; Lee, T.; Tripathy, S. *Appl. Phys. Lett.* **1998**, *72*, 2096.
(17) Barrett, C.; Natansohn, A.; Rochon, P. *J. Chem. Phys.* **1998**, *109*, 1505.
(18) Naydenova, I.; Nikolova, L.; Todorov, T.; Holme, N. C. R.; Ramanujam, P. S.; Hvilsted, S. *J. Opt. Soc. Am. B* **1998**, *15*, 1257.
(19) Pedersen, T.; Johansen, P.; Holme, N.; Ramanujam, P.; Hvilsted, S. *Phys. Rev. Lett.* **1998**, *80*, 89.
(20) Viswanathan, N. K.; Kim, D. Y.; Bian, S.; Williams, J.; Liu, W.; Li, L.; Samuelson, L.; Kumar, J.; Tripathy, S. K. *J. Mater. Chem.* **1999**, *9*, 1941.

(21) Fiorini, C.; Prudhomme, N.; de Veyrac, G.; Maurin, I.; Raimond, P.; Nunzi, J.-M. *Synth. Met.* **2000**, *115*, 121.

(22) Tripathy, S. K.; Viswanathan, N. K.; Balasubramanian, S.; Bian, S.; Li, L.; Kumar, J. In *Multiphoton and Light Driven Multielectron Processes in Organic: New Phenomena, Materials and Application*; Kajzar, F., Agranovich, M. V., Eds.; NATO Science Series 3: High Technology, Dordrecht, 2000; Vol. 79; p 421.

(23) Oliveira, O. N.; Li, L.; Kumar, J.; Tripathy, S. In *Photoreactive Organic Thin Films*; Sekkat, Z., Knoll, W., Eds.; Academic Press: San Diego, 2002; Chapter 14, p 430.

(24) Lagugne-Labarthet, F.; Buffeteau, T.; Sourisseau, C. *Appl. Phys. B* **2002**, *74*, 129.

(25) Grabiec, E.; Schab-Balcerzak, E.; Sek, D.; Sobolewska, A.; Miniewicz, A. *Thin Solid Films* **2004**, *367*, 453−454.

(26) Kwak, C. H.; Lee, S. J. *Opt. Commun.* **2000**, *183*, 547.

(27) Sek, D.; Grabiec, E.; Sobolewska, A.; Miniewicz, A. *e-Polymers* **2004**, *071*, 1.

(28) Schab-Balcerzak, E.; Sapich, B.; Stumpe, J.; Sobolewska, A.; Miniewicz, A. *e-Polymers* **2006**, *021*, 1.

(29) Sobolewska, A.; Miniewicz, A.; Grabiec, E.; Sęk, D. *Cent. Eur. J. Chem.* **2006**, *4* (2), 266.

(30) Schab-Balcerzak, E.; Grobelny, L.; Sobolewska, A.; Miniewicz, A. *Eur. Polym. J.* **2006**, *42*, 2859.

(31) Schab-Balcerzak, E.; Sobolewska, A.; Miniewicz, A.; Jurusik, J.; Jarzabek, B. Submitted for publication in *J. Polym. Sci., Part A.*

(32) Reinke, N.; Draude, A.; Fuhrmann, T.; Franke, H.; Lessard, R. A. *Appl. Phys. B* **2004**, *78*, 205.

(33) Lagugne Labarthet, F.; Buffeteau, T.; Sourisseau, C. *J. Phys. Chem. B* **1998**, *102*, 2654.

(34) Lagugne Labarthet, F.; Buffeteau, T.; Sourisseau, C. *J. Phys. Chem. B* **1999**, *103*, 6690.

(35) Chen, J. P.; Lagugne-Labarthet, F.; Natansohn, A.; Rochon, P. *Macromolecules* **1999**, *32*, 8572.

(36) Zahangir Alam, M.; Ohmachi, T.; Ogata, T.; Nonaka, T.; Kurihara, S. *Opt. Mater.* **2006**, *29*, 365.

(37) Turalski, W.; Miniewicz, A.; Bartkiewicz, S. *Adv. Mater. Opt. Electron.* **1996**, *6*, 15.

(38) Sobolewska, A.; Miniewicz, A.; Kusto, J.; Moczko, K.; Sek, D.; Schab-Balcerzak, E.; Grabiec, E.; Kajzar, F. *Proc. SPIE* **2005**, *5724*, 21.

(39) Holme, N. C. R.; Nikolova, L.; Ramanujam, P. S. *Appl. Phys. Lett.* **1997**, *70*, 1518.

(40) Eichler, H. J.; Guenter, P.; Pohl, D. W. *Laser-Induced Dynamic Gratings*; Springer-Verlag: Berlin, 1986.

(41) Lagugne Labarthet, F.; Rochon, P. L.; Natansohn, A. *Appl. Phys. Lett.* **1999**, *75*, 1377.